ICAS 2016
30th Congress of the International Council of the Aeronautical Sciences
DCC, Daejeon, Korea ; September 25-30, 2016

MODELING NONLINEAR HIGH-PRECISION UNSTEADY AERODYNAMICS FOR ADVANCED AIRCRAFT AT HIGH ANGLE OF ATTACK

Mi Baigang, Zhan Hao, Yang Meihua
College of Aeronautics, Northwestern Polytechnical University, Xi'an, China

Keywords: *state-space model; Particle Swarm Optimization (PSO); pitch rate; reduced frequency; amplitude*

Abstract

An accurate unsteady aerodynamics model at high angle of attack has an important significance to evaluate the flight characteristics of advanced flight vehicle with high maneuverability. Based on high-precision SAS numerical method, the effects of pitch rate, reduced frequency and amplitude on unsteady aerodynamics at high angle of attack have been detailed analyzed, then the factors are extracted to modify the traditional state-space model and a new state-space representation for unsteady aerodynamics up to stall range is proposed. The Particle Swarm Optimization algorithm is used to identify the unknown parameters in the model from static and dynamic CFD results. The new model and method are demonstrated by using the CFD data of a 70 degree delta wing. The results show that it is possible to analyze the unsteady aerodynamic problems in high angle of attack regime for the advanced aircraft.

1 Introduction

The requirement of flight performance for new advanced aircraft is much stricter in the increasingly complicated world pattern, and one of the remarkable characteristics for the aircraft is the ability to satisfy a variety of complex tasks with severe unsteady aerodynamic environment affected by highly maneuvering. As a result, the advanced flight vehicle tends to be mixed or large swept configuration and its flight envelope is also extended to high angle of attack region. By the way, it can be considered that the progressiveness of future new aircraft is decided by the dynamic aerodynamics at high angle of attack [1], which should be deeply analyzed.

The main causes of nonlinear unsteady aerodynamics are the separation of surface flow and the flow filed topology adjustment during highly maneuvering, and these dynamic characteristics are much more significant for advanced aircraft at high angle of attack, for the reason that various vortexes are formed and separated between wings and fuselage, while strong eddy flows generated by aircraft components rapidly change with motion parameters (attitude angles, angular velocity, acceleration .etc), which always leads to a more complicated unsteady flow flied. Moreover, the dynamic aerodynamic characteristics of advanced aircraft are also related with the time history of maneuvering, instantaneous frequency and amplitude, it is dramatically difficult for the pilot to control the aircraft coupled with flow separation and large maneuver.

For new advanced aircraft, if the aerodynamic load variation can be estimated in real-time during the dynamic maneuvering process, it will be greatly helpful to avoid the risk of flight control and improve the viability of aircraft, and the highly maneuvering will be more efficient to finish the tasks. Generally, wind tunnel experiments and flight tests are usual approaches to satisfy this demand. However, journeys are never easy for both the two roads. Due to huge economic and time costs, the methods can not be widely applied in engineering. Therefore, how to identify the nonlinear unsteady aerodynamics by limited

data becomes a new direction, this is what we usually refer to the unsteady aerodynamic modeling at high angle of attack.

Currently the limited data for modeling are mainly from wind tunnel tests. However, the relative unsteady motions are so simple that real highly maneuvers can not be well simulated. On the other hand, although several models have been developed [2-7], low precision and poor applicability are still big problems due to lack of detailed understanding of unsteady flow field.

In this paper, we choose the simulation of delta wing which has much common with new advanced aircraft as test case and focus on using a unique way to develop a new unsteady aerodynamics model at high angle of attack. Based on high-precision computational fluid dynamics (CFD) technique [8], the nonlinear and unsteady flow filed is accurately calculated and analyzed, and the factors affecting the flied at high angle of attack are detailed extracted and extended, then combined with the traditional state-space model, a new high-precision and clearly physical meaning unsteady model based on CFD can be built and further testified.

2 Numerical methods

2.1 Governing equation

The equation describing the unsteady dynamic motion is the 3D Reynolds average N-S equation expressed as:

$$\frac{\partial}{\partial t}\iiint_V \boldsymbol{W} dV + \iint_{\partial V} \boldsymbol{F}\bullet \boldsymbol{n} ds = \frac{1}{\mathrm{Re}}\iint_{\partial V} \boldsymbol{F}_v \bullet \boldsymbol{n} ds \qquad (1)$$

Where V is the control volume, $W=(\rho,\rho u,\rho v,\rho w,\rho E)^T$ is the vector of conserved variables, ρ is the density and u, v and w are the components of velocity given by the Cartesian velocity vector $U=(u,v,w)^T$. The total energy per unit mass is E. $\mathbf{F}$ denote the inviscid component of the flux vectors, while $\mathbf{F}_v$ is the viscous flux vector which contains terms of the heat flux and viscous forces exerted on the body. Re is the Reynolds number.

2.2 SAS calculating model

The model used in this paper is the Scale-Adaptive Simulation (SAS) [9] which is an improved URANS formulation and allows the resolution of the turbulent spectrum in unstable flow condition. This concept is based on the introduction of the von Karman length-scale into the turbulence scale equation. The information provided by the von Kaman length-scale allows SAS models to dynamically adjust to resolved structures in a URANS simulation, which results in an LES-like behavior in unsteady regions of the flow field. At the same time, the model provides standard RANS capabilities in stable flow regions. The SAS method can save costs compare to DES/LES, while it improves the accuracy of vortex simulation at high angle of attack, therefore this method has been widely concerned.

The SST-SAS model in this paper is modified by adding an additional source term Q_{SAS} in standard $k-\omega$ SST model, expressed as

$$\frac{\partial \rho t}{\partial t}+\frac{\partial}{\partial x_i}(\rho u_i k)=G_k-\rho c_\mu k\omega+\frac{\partial}{\partial x_j}\left[(\mu+\frac{\mu_t}{\sigma_k})\frac{\partial k}{\partial x_j}\right] \qquad (2)$$

$$\frac{\partial \rho\omega}{\partial t}+\frac{\partial}{\partial x_i}(\rho u_i\omega)=\alpha\frac{\omega}{k}G_k-\rho\beta\omega^2+Q_{SAS}+\frac{\partial}{\partial x_i}\left[(\mu+\frac{\mu_t}{\sigma_\omega})\frac{\partial\omega}{\partial x_j}\right]+(1-F_1)\frac{2\rho}{\sigma_{\omega,2}}\frac{1}{\omega}\frac{\partial k}{\partial x_j}\frac{\partial\omega}{\partial x_j} \qquad (3)$$

$$Q_{SAS}=\max[\rho\zeta_2\kappa S^2(\frac{L}{L_{vk}})^2-C\cdot\frac{2\rho k}{\sigma_\varphi}\max(\frac{|\nabla\omega|^2}{\omega^2},\frac{|\nabla k|^2}{k^2}),0] \qquad (4)$$

$$L_{vk}=\frac{\kappa\sqrt{2S_{ij}S_{ij}}}{\sqrt{\left(\nabla^2 u\right)^2+\left(\nabla^2 v\right)^2+\left(\nabla^2\omega\right)^2}} \qquad (5)$$

$$L=\sqrt{k}/(c_\mu^{1/4}\cdot\omega) \qquad (6)$$

Where L the length scale of the modeled turbulence, and L_{vk} is a three-dimensional generalization of the classic boundary layer definition.

3 Unsteady aerodynamics modeling

Several models has been developed for unsteady aerodynamics at high angle of attack in the past decades, such as the nonlinear algebraic model, indicial response method, state-space model and

the intelligent algorithm based on fuzzy logic or neural network. Among which the state-space model has more clear physical meaning than others, and can be easily coupled with control and dynamics to further analyze the aerodynamics at high angle of attack, so this model draws a lot of attention.

3.1 Traditional state-space model

The traditional state-space model was firstly proposed and applied in aerodynamics identification by Goman in 1994. In this model, the input variables are angle of attack, sideslip angle .etc, while the unsteady aerodynamic forces and moments are output ones.

By introducing the internal variables which can be taken either in a normal way or can have the well-defined physical meaning, this model can describes the state of unsteady flow. For an airfoil with sufficient thickness, a separated flow at high angle of attack can be described by the nondimesional coordinate $\bar{x} = x/c \in [0,1]$, which gives the position of the separation point on the upper surface of the airfoil. The value $\bar{x} = 1$ corresponds to attached flow, while $\bar{x} = 0$ corresponds to leading-edge separation. Therefore, based on these assumptions one can use the following equation to describe the movement of separation point for unsteady flow conditions:

$$\tau_1 \frac{dx}{dt} + x = x_0(\alpha - \tau_2 \dot{\alpha}) \tag{7}$$

Where τ_1 is the relaxation time constant, τ_2 defines the total time delay of the unsteady effect, $x_0(\alpha)$ is the stationary value of the instantaneous separation point position expressed as

$$x_0(\alpha) = \frac{1}{1 + e^{\sigma(\alpha - \alpha^*)}} \tag{8}$$

Where α^* is the angle of attack at which the flow separation is at the mid-chord point, σ is the slope factor.

The unsteady lift can then be expressed with Talyor expansion as

$$\tau_1 \frac{dx}{dt} + x = x_0(\alpha - \tau_2 \dot{\alpha}) \tag{9}$$

$$C_y = C_y(\bar{x}, \alpha, \hat{\dot{\alpha}}) = C_{y0} + C_{y\alpha}\alpha + C_{y\hat{\dot{\alpha}}}\hat{\dot{\alpha}} + \frac{1}{2}[C_{y\alpha^2} + 2C_{y\alpha\hat{\dot{\alpha}}}\alpha\hat{\dot{\alpha}} + C_{y\hat{\dot{\alpha}}^2}\hat{\dot{\alpha}}^2] \tag{10}$$

Where C_{y0} is the lift coefficient when α and $\dot{\alpha}$ equal zero, and the derivatives in Eq. (10) are functions of $\bar{x}$, that is

$$C_{y\alpha}(\bar{x}) = a_1 + b_1\bar{x} + c_1\bar{x}^2 \tag{11}$$

$$C_{y\hat{\dot{\alpha}}}(\bar{x}) = a_2 + b_2\bar{x} + c_2\bar{x}^2 \tag{12}$$

$$C_{y\alpha^2}(\bar{x}) = 2(a_3 + b_3\bar{x} + c_3\bar{x}^2) \tag{13}$$

$$C_{y\alpha\hat{\dot{\alpha}}}(\bar{x}) = a_4 + b_4\bar{x} + c_4\bar{x}^2 \tag{14}$$

$$C_{y\hat{\dot{\alpha}}^2}(\bar{x}) = 2(a_5 + b_5\bar{x} + c_5\bar{x}^2) \tag{15}$$

The state-space model can be also used to identify aerodynamics of more complicated configuration. However, the separated point equation loses its physical meaning at the time due to the strongly coupling flow filed characteristics, and it represents a global parameter to estimate the unsteady aerodynamics. Furthermore, since the nonlinear and hysteresis characteristics are also affected by the pitch rate, amplitude and reduced frequency, and they respectively describe the change of local angle of attack, the maximum angle of attack and the instantaneous pitch rate in the unsteady motion, which are reflected by the internal variables. Thus, the traditional model should be modified.

3.2 State-space model modification

The traditional model only considers the angle of attack, which can not relatively completely analyze the unsteady flow flied characteristics. In this part, we use the high-precision CFD method to extract the factors and correct the state-space model.

3.2.1 Pitch rate q

The pitch rate q has the same formulation with rate of angle of attack $\dot{\alpha}$ at constant free stream velocity and this value can be more efficient to describe the dynamic damping at high angle of attack, this can be clear concluded from traditional dynamic derivative model since the pitching moment produced by the additional aerodynamic forces always seems to impede the motion.

3.2.2 Reduced frequency k

The reduced frequency defined as $k = \omega c / 2V$ is the ratio between the vibration frequency and the velocity of free stream. Even though the reduced frequency can represents the variations of rate of angle of attack or pitch rate, it is not exactly the same as nondimensinonal pitch rate, that is

$$\dot{\alpha} = q = \frac{2kV}{c}\alpha_m \cos(\frac{2kV}{c}t) \qquad (16)$$

Fig.1 shows the unsteady lift and pitching moment coefficients of the VFE-2 model at high angle of attack with different reduced frequencies [10], and the results indicate that both the hysteresis loop areas and the absolute values of aerodynamic forces at the maximum angle of attack increase with the reduced frequency. Moreover, the vortex evolutions in pitch up and down are also heavily affected, which leads to more significant dynamic delays.

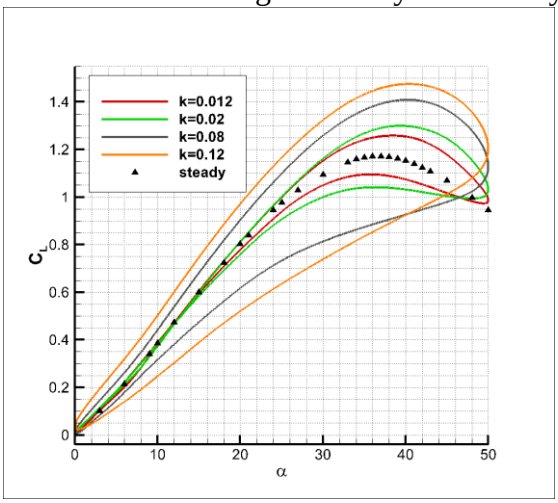

(a) Lift coefficients

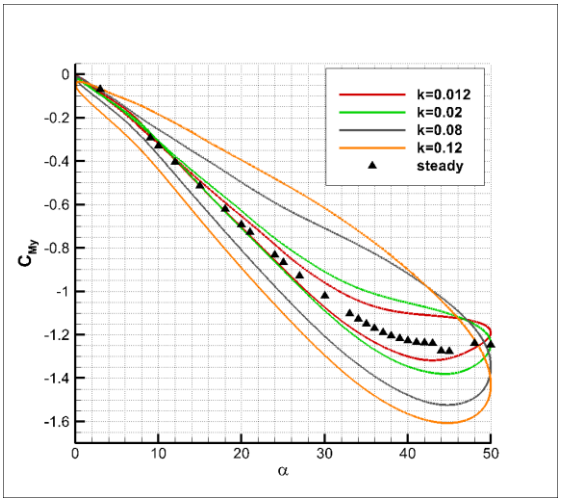

(b) Pitching moment coefficients

Fig. 1 Unsteady aerodynamics with different reduced frequencies

3.2.3 Amplitude α_m

The amplitude α_m determines the instantaneous maximum angle of attack which is closely related to separation characteristic, thus the effect of α_m should be considered. Actually similar to reduced frequency, amplitude also defines the variations of rate of angle of attack or pitch rate during the unsteady motion, showed as

$$\dot{\alpha} = q = \omega\alpha_m \cos(\omega t) \qquad (17)$$

The amplitude can affect the angle of attack and derivatives without changing the movement period. Fig.2 is the unsteady aerodynamics of VFE-2 model with different amplitudes at high angle of attack. The results show that objective dynamic delay is produced with the comparison between dynamic and static aerodynamic data, and this effect becomes much more apparent as the amplitude increases, which leads to larger dynamic increments of aerodynamic forces and moments. In detail, the amplitude determines the flow patterns in unsteady process, and larger amplitude means the motion will cross more patterns.

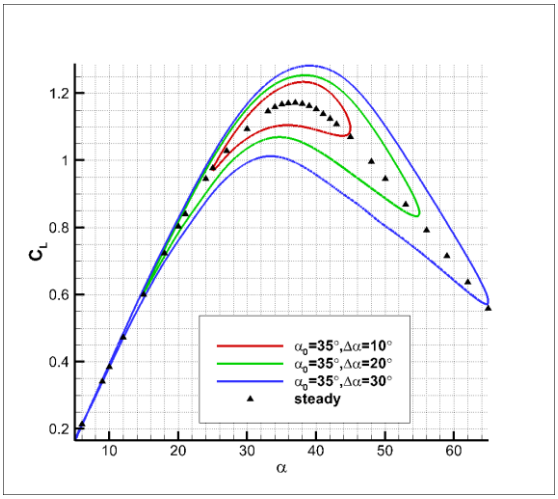

(a) Lift coefficients

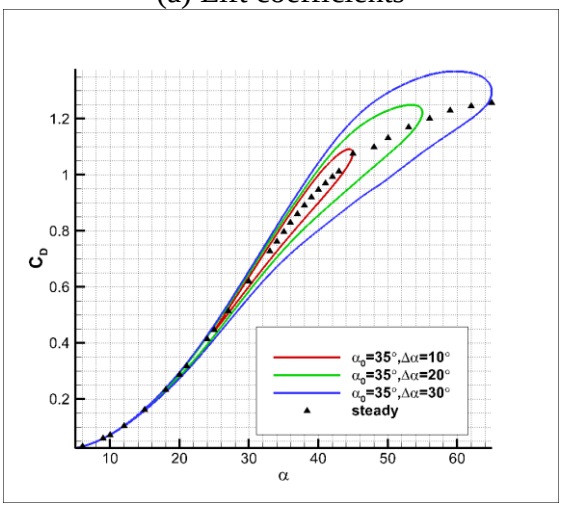

(b) Drag coefficients

Fig.2 Unsteady aerodynamics with different amplitudes

Furthermore, the pitch rate q, reduced frequency k and amplitude α_m which heavily affect the unsteady aerodynamics at high angle of attack should be considered to modify the traditional state-space model. Firstly, due to the fact that q has the same form with $\dot{\alpha}$, $\tau_2\dot{\alpha}$ can be extend to $\tau_2(\dot{\alpha}+q)$ in the separation equation without adding more estimating parameters. Then considering the relation among k, α_m and $\dot{\alpha}$

$$\Delta\alpha = \alpha_m \sin(\omega t) \tag{18}$$

$$\dot{\alpha} = q = \omega\alpha_m \cos(\omega t) \tag{19}$$

The nondimensional form of $\dot{\alpha}$ is

$$\hat{\dot{\alpha}} = \frac{\dot{\alpha} l}{2V} = \hat{q} = \frac{ql}{2V} = \frac{\omega l}{2V}\alpha_m \cos(\omega t) = k\alpha_m \cos(\omega t) \tag{20}$$

Therefore, the state equation of separation flow can be further modified as

$$\tau_1 \frac{dx}{dt} + x = x_0(\alpha - \tau_2(\dot{\alpha}+q) - \tau_3 k\alpha_m) \tag{21}$$

Fig.3 is the diagram of vortex separation location in Eq. (21). Finally the modified model with CFD analysis can be developed, expressed as

$$\tau_1 \frac{dx}{dt} + x = x_0(\alpha - \tau_2(\dot{\alpha}+q) - \tau_3 k\alpha_m) \tag{22}$$

$$C_y = C_y(\bar{x}, \alpha, \hat{\dot{\alpha}}) = C_{y0} + C_{y\alpha}\alpha + C_{y\hat{\dot{\alpha}}}\hat{\dot{\alpha}} + \frac{1}{2}[C_{y\alpha^2} + 2C_{y\alpha\hat{\dot{\alpha}}}\alpha\hat{\dot{\alpha}} + C_{y\hat{\dot{\alpha}}^2}\hat{\dot{\alpha}}^2] \tag{23}$$

$$C_{y\alpha}(\bar{x}) = a_1 + b_1\bar{x} + c_1\bar{x}^2 \tag{24}$$

$$C_{y\hat{\dot{\alpha}}}(\bar{x}) = a_2 + b_2\bar{x} + c_2\bar{x}^2 \tag{25}$$

$$C_{y\alpha^2}(\bar{x}) = 2(a_3 + b_3\bar{x} + c_3\bar{x}^2) \tag{26}$$

$$C_{y\alpha\hat{\dot{\alpha}}}(\bar{x}) = a_4 + b_4\bar{x} + c_4\bar{x}^2 \tag{27}$$

$$C_{y\hat{\dot{\alpha}}^2}(\bar{x}) = 2(a_5 + b_5\bar{x} + c_5\bar{x}^2) \tag{28}$$

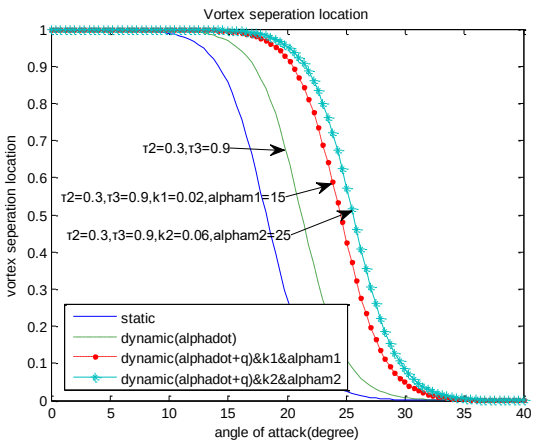

Fig.3 Vortex separation location with modified model

4 Parameter identification

4.1 Output equations

The lift, drag and pitch moment coefficients are the outputs of the system of interest in the new model. They are still functions of state $x(t)$ and inputs: $\alpha(t)$ and $\hat{q}(t)$ based on Eq. (29).

$$C_i = C_i(x, \alpha, \hat{q}) \tag{29}$$

Where C_i represents C_l, C_d and C_m.

We still use Taylor series expansions of Eq. (01) but in order to resemble the current of stability derivatives, we do the expansions in terms of α and $\hat{q}$ around the origin, while holding state x fixed. Then we can write

$$\begin{aligned} C_i &= C_i(x, \alpha, \hat{q}) = C_{i0} + (\frac{\partial C_i}{\partial \alpha})\alpha + (\frac{\partial C_i}{\partial \hat{q}})\hat{q} \\ &+ \frac{1}{2}\left[(\frac{\partial^2 C_i}{\partial \alpha^2})\alpha^2 + (\frac{\partial^2 C_i}{\partial \hat{q}^2})\hat{q}^2 + 2(\frac{\partial^2 C_i}{\partial \alpha \partial \hat{q}})\alpha\hat{q} \right] + \cdots \end{aligned} \tag{30}$$

Since all the partial derivatives are evaluated at $(\alpha, \hat{q}) = (0,0)$, they only depend on state variable x. C_{i0} is the aerodynamic coefficient when α and $\hat{q}$ equal zero. At such conditions, the flow is generally attached. Therefore we can treat C_{i0} as a constant, independent of x. Generally the term up to second derivatives should be retained for sufficient accuracy, so the aerodynamic coefficient can be expressed as

$$\begin{aligned} C_i &= C_i(x, \alpha, \hat{q}) = C_{i0} + C_{i\alpha}(x)\alpha + C_{i\hat{q}}(x)\hat{q} \\ &+ C_{i\alpha^2}(x)\alpha^2 + C_{i\hat{q}^2}(x)\hat{q}^2 + C_{i\alpha\hat{q}}(x)\alpha\hat{q} \end{aligned} \tag{31}$$

All the derivatives are functions of state variable x, that is

$$C_{i\alpha}(\bar{x}) = a_1 + b_1\bar{x} + c_1\bar{x}^2 \tag{32}$$

$$C_{i\hat{\alpha}}(\bar{x}) = a_2 + b_2\bar{x} + c_2\bar{x}^2 \tag{33}$$

$$C_{i\alpha^2}(\bar{x}) = 2(a_3 + b_3\bar{x} + c_3\bar{x}^2) \tag{34}$$

$$C_{i\alpha\hat{\alpha}}(\bar{x}) = a_4 + b_4\bar{x} + c_4\bar{x}^2 \tag{35}$$

$$C_{i\hat{\alpha}^2}(\bar{x}) = 2(a_5 + b_5\bar{x} + c_5\bar{x}^2) \tag{36}$$

4.2 Parameter estimation

Several parameters: $\alpha^*, \sigma, \tau_1, \tau_2, \tau_3, C_{i0}, a_i$ in the new state-space model should be determined, among which α^*, σ can be calculated with static data, while the others like τ_1, τ_2, τ_3 should be identified by using a series of dynamic aerodynamic data at high angle of attack. The general method used is gradient-type algorithm, such as the Newton- Raphson and conjugate gradient methods, however, it is not convenient to do the job because a lot of derivatives should be calculated during the identification. In this paper, we adopt the particle swarm optimization algorithm (PSO) instead of the traditional methods to identify the dynamic parameters.

In order to improve the efficiency of identification, the estimating parameters are divided into two parts. We first define the static data to obtain the parameters which is irrelevant to pitch rate. In the steady case, suppose that for a given sequence of angle of attack: $\alpha_j (j = 1,2,...,l)$, the CFD calculation results at these points are $\hat{C}_i(\alpha_j), (j = 1,2,...,l)$, and the output coefficients by using the new model are $C_i = C_i(x, \alpha_j) = C_{i0} + C_{i\alpha}(x)\alpha_j + C_{i\alpha^2}(x)\alpha_j^2$. In such a case, the mean-square error can be defined as $\varepsilon_{static} = \sum_{j=1}^{l} [C_i(x, \alpha_j) - \hat{C}_i(\alpha_j)]^2$, which is also the target function in PSO method.

Combined with the results calculated from static data, we can use the similar method to further identify the other dynamic parameters. Suppose that for given time history of inputs at separation flow conditions: $(\alpha(t), \hat{q}(t), 0 \le t \le T)$, the corresponding CFD results are $\hat{C}_i(t_j), (j = 1,2,...,n)$, while the outputs at the sample points are described as

$$\begin{aligned} C_i(t_j) &= C_i(x, \alpha(t_j), \hat{q}(t_j)) = C_{i0} + C_{i\alpha}(x)\alpha(t_j) \\ &+ C_{i\hat{q}}(x)\hat{q}(t_j) + C_{i\alpha^2}(x)\alpha(t_j)^2 + C_{i\hat{q}^2}(x)\hat{q}(t_j)^2 \\ &+ C_{i\alpha\hat{q}}(x)\alpha(t_j)\hat{q}(t_j) \end{aligned} \tag{37}$$

The mean-square error or the target function of dynamic identification is

$$\varepsilon_{dynamic} = \sum_{j=1}^{n} [C_i(t_j) - \hat{C}_i(t_j)]^2 \tag{38}$$

From the two steps PSO calculation, finally we can get the identification results.

5 Model validation

5.1 Computational model and mesh

In this part a 70 degree delta wing with sharp edge is used to demonstrate the performance of the new modified state-space model [11]. The geometry is shown in Fig.4, the root chord and wing span are respectively 0.762m and 0.5548m. The model has 25 degree leading and trailing edge bevels.

The H-H type mesh for CFD computing is generated by ANSYS ICEM CFD software with a total number of 4.5 million points, and the largest y^+ does not exceed the value of 1.0. The volume and surface mesh can be seen in Fig.5.

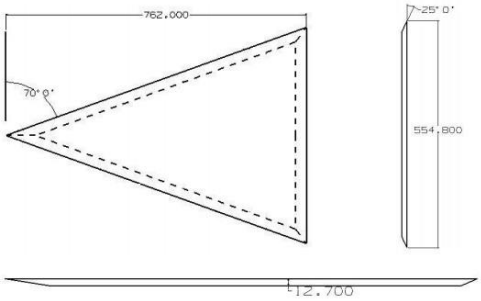

Fig.4 Computational model of the delta wing

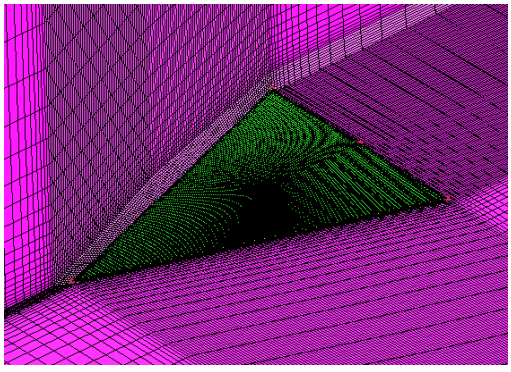

(a) Volume mesh

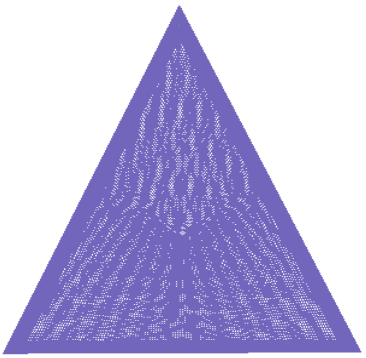

(b) Surface mesh

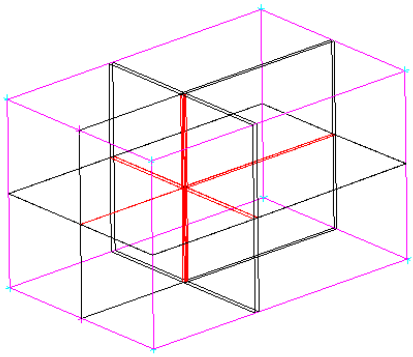

(c) Mesh topology

Fig.5 Computational mesh

5.2 Steady cases testing

We firstly use SAS method to test the steady cases of the delta wing. Calculations are performed at a freestream Mach number $Ma = 0.3$ and several angles of attack. The Reynolds number based on the root chord is one million. Fig.6 shows the lift coefficients at these angles of attack, which indicates good agreement with the wind tunnel data [11]. The locations or trajectories of the leading-edge vortex from the SAS numerical solution for $\alpha = 30^\circ$ are shown in Fig.7. Two orthogonal views of the wing are given in Fig.8 to define the primary vortex location relative to the wing. The computational solutions show excellent agreement with each other and the experimental data along the axis.

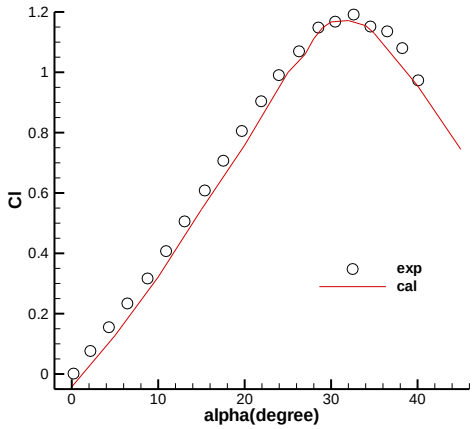

Fig.6 Lift coefficients

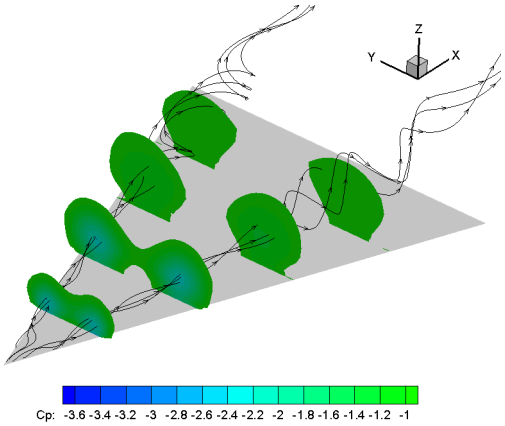

Fig.7 Vortex indicated with particle traces at $\alpha = 30^{\circ}$

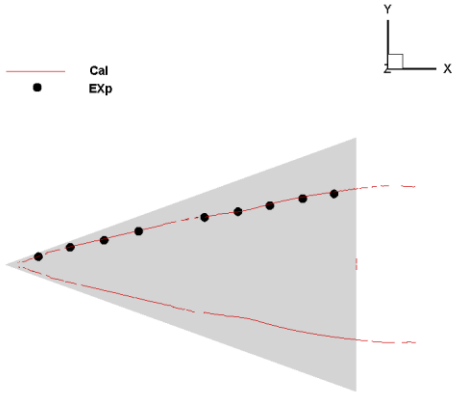

(a) Vortex locations (planform view)

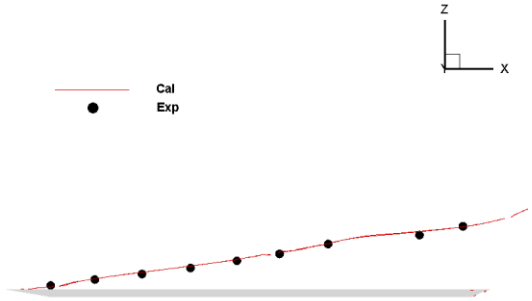

(b) Vortex locations (side view)

Fig.8 Vortex locations at $\alpha = 30^{\circ}$

5.3 Unsteady aerodynamics validation

The unsteady aerodynamics calculation is completed by using the rigid dynamic mesh technique, and the computational conditions are the same with steady cases. Based on steady result at the initial angle of attack $\alpha_0 = 30^{\circ}$, the unsteady aerodynamics is proposed with a sinusoidal motion described as

$$\alpha = \alpha_0 + \alpha_m \sin(\omega t) = 30^{\circ} + 30^{\circ} \sin(11.6141732t) \quad (39)$$

Where α_m is the amplitude of the unsteady motion, and the reduced frequency is $k = \omega C_r / 2V = 0.05$.

The new modified state-space model is applied to testify both the static and dynamic aerodynamics of the delta wing. Combined with PSO algorithm, we can finally obtain the steady and unsteady outputs of the model. Fig.9 shows the static lift, drag and pitch moment coefficients at the given angles of attack, while Figs. 10, 11 and 12 respectively give the unsteady ones. From the plots, we can see that the model responses match the numerical data from SAS method very well for all the cases.

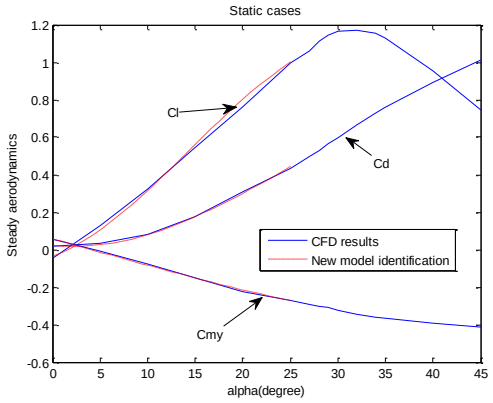

Fig. 9 Steady data with CFD and new model

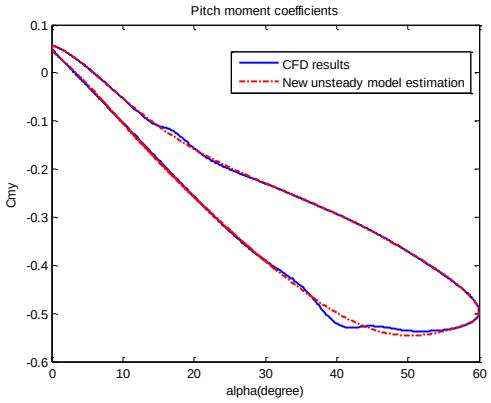

Fig. 12 Unsteady pitch moment coefficients with CFD and new model

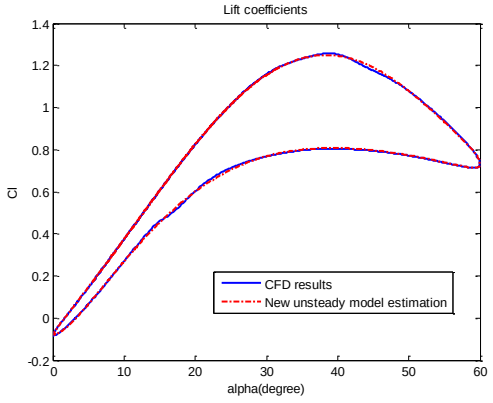

Fig. 10 Unsteady lift coefficients with CFD and new model

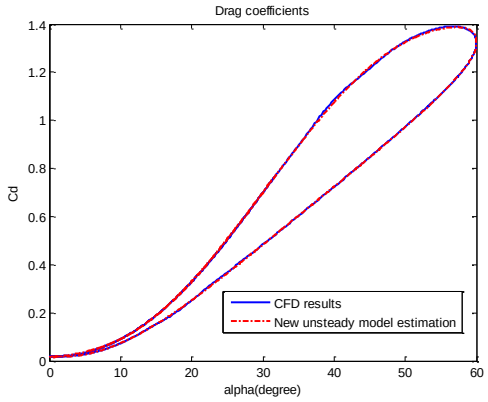

Fig. 11 Unsteady drag coefficients with CFD and new model

6 Conclusion

Combined with high-precision CFD methods, a new state-space model is presented in this paper to describe the unsteady aerodynamic characteristics at high angle of attack. From which several conclusions are summarized as follows:

1) By using the computational models like SAS or DES/LES method, the static or dynamic flow fields can be much more accurately simulated, which will be beneficial to better understand the aerodynamics and develop unsteady model at high angle of attack.

2) The pitch rate has the same form as well as rate of angle of attack since the freestream is unchanged, and both of these factors have similar effects on the unsteady aerodynamics. Moreover, the reduced frequency and amplitude can change the instantaneous pitch rate during the dynamic process, and the flow separation could be affected.

3) The new model fully considers the factors of pitching rate, reduced frequency and amplitude with CFD analysis, and it can be used to model the static and dynamic aerodynamics which has been validated by the 70 degree delta wing.

The new model proposed in this paper is still need to be investigated as the complexity of flow field in high angle of attack regime. It is limited by long time calculation, a large number of estimating parameters and insufficiently precise flow field analysis. Thus we will modify

this model in the future and extend it to lateral directional unsteady aerodynamics modeling at high angle of attack.

Acknowledgements

This research was supported by the Aeronautical Science Foundation of China (Grant No. 2015ZA53013)

References

[1] Tobak M and Chapman G T. Modeling aerodynamic discontinuities and the onset of chaos in flight dynamic systems. *Annals of Telecommunications*, Vol. 42, No. 5, pp 300-314, 1986.

[2] Lin G F and Lan C E. A generalized dynamic aerodynamic coefficient model for flight dynamics application. Atmospheric Flight Mechanics Conference, New Orlea, LA, pp 377-391, 1997.

[3] Goman M and Khrabrov A. State-space representation of aerodynamic characteristic of an aircraft at high angles of attack. *Journal of Aircraft*, Vol. 31, No.1, pp 1109-1115, 1994.

[4] Daniel A. A. and Jeremy A. S. Nonlinear modeling of unsteady aerodynamics at high angle of attack. *Atmospheric Flight Mechanics Conference and Exhibit*, Providence, Rhode Island, pp 1-19, 2004.

[5] Maziar S. H., Scott T. M. and Clarence W. R. Unsteady aerodynamic response modeling: a parameter-varying approach. *53rd AIAA Aerospace Sciences Meeting*, Kissimmee, Florida, pp 1-14, 2015.

[6] Erik G. R. and De B. Reduced-order modeling of continuous-time state-space unsteady aerodynamics. *53rd AIAA Aerospace Sciences Meeting*, Kissimmee, Florida, pp 1-14, 2015.

[7] Ghoreyshi M. and Russell M. C. Challenges in the aerodynamics modeling of an oscillating and translating airfoil at large incidence angles. *Aerospace Science and Technology*, Vol. 28, No. 1, pp 176-190, 2013.

[8] Jianghua K. and Jack R. E. RANS and hybrid LES/RANS simulations of flow under a dynamically pitching NACA0012 airfoil. *51st AIAA Aerospace Sciences Meeting*, Grapevine, Texas, pp 1-28, 2015.

[9] Menter F. and Egorov Y. The Scale-adaptive simulation method for unsteady turbulent flow predictions. Part 1: theory and model description. *Journal Flow Turbulence and Combustion*, Vol.1, No.2, pp 113-138, 2010.

[10] AVT-080 Report. RTO & Springer Verlag, 2007.

[11] Shreelant A., Raymond M. B. and Brian A. R. Numerical investigation of vortex breakdown on a delta wing. *AIAA Journal*, Vol. 30, No.3, pp 584-591, 1992.

Contact Author Email Address

mibaigang@163.com

Copyright Statement